

# Copper Alters Aggregation Behavior of Prion Protein and Induces Novel Interactions between Its N- and C-terminal Regions<sup>§</sup>

Received for publication, May 27, 2011, and in revised form, August 29, 2011. Published, JBC Papers in Press, September 7, 2011, DOI 10.1074/jbc.M111.265645

Abhay Kumar Thakur<sup>†1</sup>, Atul Kumar Srivastava<sup>§</sup>, Volety Srinivas<sup>‡</sup>, Kandala Venkata Ramana Chary<sup>§</sup>, and Chintalagiri Mohan Rao<sup>†2</sup>

From the <sup>†</sup>Centre for Cellular and Molecular Biology, Council of Scientific and Industrial Research, Uppal Road, Hyderabad 500 007 and the <sup>§</sup>Department of Chemical Sciences, Tata Institute of Fundamental Research, Homi Bhabha Road, Colaba, Mumbai 400 005, India

**Background:** Role of copper as an attenuator or facilitator in prion diseases is controversial.

**Results:** Copper-bound PrP does not aggregate at physiological temperature and shows two novel interactions between its N- and C-terminal domains.

**Conclusion:** Copper may act as an attenuator in prion diseases and induces novel long range inter-domain interactions in PrP.

**Significance:** This study might help in understanding the role of copper in prion diseases.

Copper is reported to promote and prevent aggregation of prion protein. Conformational and functional consequences of Cu<sup>2+</sup>-binding to prion protein (PrP) are not well understood largely because most of the Cu<sup>2+</sup>-binding studies have been performed on fragments and truncated variants of the prion protein. In this context, we set out to investigate the conformational consequences of Cu<sup>2+</sup>-binding to full-length prion protein (PrP) by isothermal calorimetry, NMR, and small angle x-ray scattering. In this study, we report altered aggregation behavior of full-length PrP upon binding to Cu<sup>2+</sup>. At physiological temperature, Cu<sup>2+</sup> did not promote aggregation suggesting that Cu<sup>2+</sup> may not play a role in the aggregation of PrP at physiological temperature (37 °C). However, Cu<sup>2+</sup>-bound PrP aggregated at lower temperatures. This temperature-dependent process is reversible. Our results show two novel intra-protein interactions upon Cu<sup>2+</sup>-binding. The N-terminal region (residues 90–120 that contain the site His-96/His-111) becomes proximal to helix-1 (residues 144–147) and its nearby loop region (residues 139–143), which may be important in preventing amyloid fibril formation in the presence of Cu<sup>2+</sup>. In addition, we observed another novel interaction between the N-terminal region comprising the octapeptide repeats (residues 60–91) and helix-2 (residues 174–185) of PrP. Small angle x-ray scattering studies of full-length PrP show significant compactness upon Cu<sup>2+</sup>-binding. Our results demonstrate novel long range inter-domain interactions of the N- and C-terminal regions of PrP upon Cu<sup>2+</sup>-binding, which might have physiological significance.

Prion protein (PrP)<sup>3</sup> is involved in transmissible spongiform encephalopathies, a group of diseases such as Creutzfeldt-Jakob disease, Kuru, Fatal Familial Insomnia, and Gerstmann-Straussler-Scheinker syndrome, characterized by neurodegeneration, spongiform cerebral tissue, and amyloid plaques. Such diseases are caused by the conformational transition of  $\alpha$ -helix-rich cellular prion protein (PrP<sup>C</sup>) to the  $\beta$ -sheet-rich scrapie prion protein (PrP<sup>Sc</sup>) (1). Copper ions (Cu<sup>2+</sup>) appear to have a significant role in such conformational transition (2). PrP exhibits strong binding toward Cu<sup>2+</sup> with nano- to femtomolar affinity (3–5). Cu<sup>2+</sup>-binding sites are reported in the flexible N-terminal region (residues 23–120); four of them are present in the octapeptide repeats (residues 60–91) and one located at His-96 and His-111 (6–8) (residues are numbered according to the human PrP sequence). An additional Cu<sup>2+</sup>-binding site at His-187 has also been recognized in the C-terminal region of PrP (9–12).

Although the functional implication of Cu<sup>2+</sup>-binding to PrP is not yet clear, it is believed that Cu<sup>2+</sup> is an important factor (as a facilitator or an attenuator) in prion diseases. Cu<sup>2+</sup>-binding induces conformational changes leading to reduction in the helical content and an increase in the  $\beta$ -sheet content especially in the region 90–120 (13), which partially overlaps with the well established amyloidogenic stretch 106–126 (14). Cu<sup>2+</sup> has also been shown to induce conformational changes and increased stability in the octapeptide repeats of PrP (15, 16).

Cu<sup>2+</sup> is shown to convert PrP<sup>C</sup> from brain homogenates (2) and aged recombinant PrP (17) to protease-resistant and detergent-insoluble aggregates. However, these aggregates are structurally distinct from the scrapie prion protein (PrP<sup>Sc</sup>). Expansion of octapeptide repeats has been suggested to cause an early onset of the prion disease (18, 19). In contrast, several studies show compelling evidence on the inhibitory role of Cu<sup>2+</sup> on the amyloid formation of PrP *in vitro* (20–23). *In vivo* studies of Cu<sup>2+</sup>-binding to PrP are also not unequivocal. One study

<sup>3</sup> The abbreviations used are: PrP, prion protein; SAXS, small angle x-ray scattering; ITC, isothermal calorimetry; EOM, ensemble optimization method.

<sup>§</sup> The on-line version of this article (available at <http://www.jbc.org>) contains supplemental Figs. S1–S6 and Table S1.

<sup>1</sup> Recipient of a senior research fellowship from Council of Scientific and Industrial Research, New Delhi, India.

<sup>2</sup> Recipient of a J. C. Bose National Fellowship from the Department of Science and Technology, Government of India. To whom correspondence should be addressed. Tel.: 91-40-2716-0789; Fax: 91-40-2716-0310, 0311, or 0591; E-mail: mohan@cmb.res.in.

## Cu<sup>2+</sup>-PrP, Aggregation, and N- and C-terminal Interactions

reports the delay in the onset of prion disease upon removal of Cu<sup>2+</sup> by chelation (24), whereas a different study shows that Cu<sup>2+</sup>-depleted diet enhances prion disease (25). Thus, the nature and consequences of interaction of Cu<sup>2+</sup> with PrP, both *in vitro* and *in vivo*, appear to be a complex phenomenon that remains to be investigated.

Conformational studies on binding of Cu<sup>2+</sup> to PrP *in vitro* have been performed using peptides (26–28) or truncated variants of PrP (29–31) and at nonphysiological temperatures (2, 10, 13–17) and in water or buffers of low ionic strength (3, 9, 13, 32–34). We have used full-length PrP(23–231) to investigate conformational changes and aggregation upon Cu<sup>2+</sup>-binding at physiological temperature (37 °C). We find that Cu<sup>2+</sup>-bound PrP undergoes unusual temperature-dependent reversible aggregation. Interestingly, it aggregates at lower temperatures and resolubilizes as the temperature is raised. Our investigations using isothermal calorimetry (ITC), NMR, and small angle x-ray scattering (SAXS) provide insight into thermodynamic and conformational aspects of this process. Based on our study, we propose the involvement of the interaction of helix-2 and the octapeptide repeats region in the aggregation process. Our results reveal two novel interactions between the flexible N- and the C-terminal regions of PrP upon Cu<sup>2+</sup>-binding as follows: (i) between the N-terminal region and helix-1 (residues 144–147) and its nearby loop region (residues 139–143) and (ii) between the N-terminal region (residues 60–91) and helix-2 (residues 174–185) of PrP. We believe these observations have physiological implications.

### EXPERIMENTAL PROCEDURES

All chemicals and reagents were of analytical or ultra pure grade. Isopropyl 1-thio-β-D-galactopyranoside was obtained from Bangalore Genei (India), and urea was procured from United States Biochemical (Cleveland, OH), and ampicillin was purchased from Biochem Pharmaceutical Industries Ltd. (India). Protease inhibitor mixture was from Roche Diagnostics; NaCl and glycine were from Qualigens, Fine Chemicals (India); CuSO<sub>4</sub> was from Sisco Research Laboratories Pvt. Ltd. (Mumbai, India). Nickel-nitrilotriacetic acid matrix was obtained from Qiagen (GmbH, Hilden, Germany). Other chemicals or reagents were from Sigma. Water used in all reactions was obtained from MilliQ, Millipore (Bedford, MA).

**Cloning, Expression, and Purification of Prion Protein Variants**—We have cloned, expressed, and purified mouse PrP(23–231) as described earlier (35). PrP(90–231) was cloned into pET21a vector after PCR amplification from PrP(23–231)-pET21a template using gene-specific primers (forward primer TGGCATATGGGCAAGGAGGGGGTAC and reverse primer GCTTTCGAATCAGCTGGATCTTCTCCCG). Inserts in pMOS blue vector (Novagen) were digested with NdeI and HindIII and ligated by T4-DNA polymerase (Promega) in pET21a vector. *Escherichia coli* DH5α strain was transfected with the plasmid constructs. Positive colonies were screened with the help of ampicillin. The sequence of this construct was verified using 3700ABI automated DNA sequencer. MoPrP(90–231) (pET21a vector) was expressed in *E. coli* Rosetta DE3. After 12 h of induction, cells were harvested, lysed, and centrifuged. The insoluble pellet was washed and

dissolved in 8 M urea and 10 mM reduced glutathione and bound to nickel-nitrilotriacetic acid matrix. On-column oxidative folding of PrP was done by slow removal of the denaturant and the reducing agent. Protein was eluted in 50 mM imidazole. The eluted protein was extensively dialyzed against MilliQ water and then concentrated. Aliquots of protein were stored at –70 °C. The protein concentrations were estimated using the extinction coefficient of 2.70 and 1.70 at 280 nm for 1 mg/ml solutions of PrP(23–231) and PrP(90–231), respectively. The purity of the protein was checked using SDS-PAGE and found to be free of any contaminants.

**PrP Preparations for Spectroscopic Measurements**—Scattering experiments were performed in 20 mM sodium phosphate buffer (pH 7.4) and 100 mM NaCl, unless otherwise specified. For ITC, SAXS, dynamic light scattering, sedimentation velocity, and NMR experiments, PrP in water with pH 7.4 maintained by dilute NaOH solution was used to avoid aggregation. At low protein (~0.25 mg/ml) concentrations, the reversible aggregation was not noticeable. However, at higher concentrations up to 2 mg/ml in water (pH 7.4), reversible aggregation was observed below 22 °C.

**Cu<sup>2+</sup>-binding Studies**—For all Cu<sup>2+</sup>-binding studies, including aggregation, NMR, SAXS, sedimentation velocity, and ITC experiments, Cu<sup>2+</sup> was complexed with glycine in a 1:4 molar ratio to form Cu-(Gly)<sub>2</sub> complex (referred to as Cu<sup>2+</sup> everywhere in the text) to avoid any hydroxide formation. The Cu-(Gly)<sub>2</sub> complex was maintained at pH 6.0 to avoid drastic change in pH of PrP (water, pH 7.4) upon titration in ITC experiments. After titration, no significant change in pH was observed. Except for ITC, all the binding studies were done using 6 M eq of Cu<sup>2+</sup>.

**Scattering Studies**—Scattering measurements were monitored using Spectrofluorimeter Fluorolog-3 model FL-3–22 from Horiba Jobin Yvon, Inc. Rayleigh scattering of solutions was recorded at any given temperature with excitation and emission monochromators fixed at 465 nm, and bandpasses for excitation and emission were set at 0.5 and 1 nm, respectively. Datamax software provided by the manufacturer was used to monitor scattering. The instrument takes 2.5 and 3 min to increase or decrease the sample temperatures from 15 to 37 °C, respectively. To measure the extent of reversibility, scattering was monitored at various temperatures between 37 and 15 °C and brought back to 37 °C with similar intervals.

**Isothermal Calorimetry**—Binding of Cu-(Gly)<sub>2</sub> complex with PrP(23–231) was performed using VP-ITC microcalorimeter from MicroCal, LLC. Data acquisition and analysis were done with software provided by the manufacturer. PrP(23–231) at a concentration of 0.25 mg/ml (12 μM) in water (pH 7.4) was used and 2 mM of Cu-(Gly)<sub>2</sub> was titrated against it. Each solution was filtered or centrifuged and degassed before binding experiments. Initial injection of 2 μl followed by 29 injections of 4 μl was used for binding reactions. To remove the heat of dilution generated because of injection of ligands to the protein solution in the binding reactions, base-line correction for raw isotherms was performed by subtracting average saturated values (obtained from six points) from its corresponding isotherms. For analysis, a sequential mode with four binding sites was used. Binding reactions were performed at 16, 20, 25, 30, and 37 °C.

Three reactions were done at each temperature, and averaged values are reported.

**NMR of Prion Protein**—Uniformly <sup>15</sup>N-labeled protein samples of PrP(23–231) and PrP(90–231) were prepared by growing *E. coli* cells in M9 minimal medium containing <sup>15</sup>NH<sub>4</sub>Cl as the sole source of nitrogen. Protein samples (2 mg/ml) were prepared in ultra pure water (10<sup>-18</sup> Ω<sup>-1</sup> cm<sup>-1</sup> resistivity) whose pH was maintained at 7.4. Two-dimensional <sup>15</sup>N-<sup>1</sup>H HSQC spectra were recorded for PrP(23–231) and PrP(90–231) at various temperatures ranging from 16 to 37 °C. Each <sup>15</sup>N-<sup>1</sup>H HSQC was recorded with 1024 and 128 complex points along <sup>1</sup>H and <sup>15</sup>N dimensions, respectively, using watergate sequence for water saturation, on a Bruker Avance 800 MHz NMR spectrometer equipped with a 5-mm triple-resonance cryogenic probe, whose temperature was calibrated using methanol (280–300 K). All the spectra were referenced using 4,4-dimethyl-4-silapentane-1-sulfonic acid as an external reference at 298 K and then adding the correction of 0.01 ppm/K for the temperature change. The spectra were processed with 4096 and 1024 points along <sup>1</sup>H and <sup>15</sup>N dimensions, and a window function of 60°-shifted sine square bell was used for apodization along both the dimensions using TopSpin 2.0 software. Analysis was carried out manually using computer-aided resonance assignment (CARA).

**NMR Assignments**—Prior to the assignment of the peaks in the two-dimensional <sup>15</sup>N-<sup>1</sup>H HSQC of PrP(90–231), recorded in a mixed solvent of <sup>2</sup>H<sub>2</sub>O and H<sub>2</sub>O (pH 7.4), we recorded the same spectrum at pH 7.0 for which the chemical shift information (32) is available in the BioMagResBank (code 16071) under similar buffer conditions, 5 mM phosphate buffer (pH 7.0). All the observed peaks in the pH 7.0 spectrum, totaling 128 out of 138, could be assigned by visual inspection. The missing spectral information about the 10 remaining residues belongs to the flexible part of the protein. In such an assignment, no changes were noticed in the respective chemical shifts, except for the residue Phe-141. We then assigned the <sup>15</sup>N-<sup>1</sup>H HSQC of PrP(90–231) recorded in water at pH 7.4 by comparing it with the spectral assignments made at pH 7.0. Once again, no spectral changes were noticed except for the absence of 17 more cross-peaks belonging to the unstructured part of the protein (residues 90–120). Thus, we could unambiguously assign the spectral signatures of 111 residues. Such assignments were further used to assign 85 of the observed peaks in the <sup>15</sup>N-<sup>1</sup>H HSQC of wild-type prion protein, recorded under identical experimental conditions. Among the residues, whose spectral signatures were absent in the spectrum, 28 belong to the unstructured polypeptide stretch (residues 90–120), and the residues Val-166–Asn-171, Arg-230, and Ser-231, all belonging to the globular domain of the protein.

**Sedimentation Velocity Measurements**—Sedimentation velocity measurements were performed using Optima XL-I analytical ultracentrifuge (Beckman Coulter, Fullerton, CA). Prion protein samples (2 mg/ml (pH 7.4), conditions identical to those used in NMR experiments), with and without Cu<sup>2+</sup>, were subjected to centrifugation at 58,000 rpm (~240,000 × *g*) at 37 °C, using An60Ti rotor with an aluminum center piece. The protein boundary was scanned at 1-min intervals for 8 h by interference measurements using 30-milliwatt 660 nm laser

diode. The sedimentation coefficient *s*<sub>20,w</sub> and molecular mass of the protein were calculated using the program SEDFIT (36), which uses nonlinear regression fitting of the sedimenting boundary profile with the Lamm Equation 1,

$$\frac{dc}{dt} = \frac{1}{r} \times \frac{d}{dr} \left( rD \frac{dc}{dr} - s\omega^2 r^2 \cdot c \right) \quad (\text{Eq. 1})$$

which describes the concentration distribution *c*(*r*,*t*) of a species with sedimentation coefficient *s* and diffusion coefficient *D* in a sector-shaped volume and in the centrifugal field  $\omega^2 r$ .

**SAXS Studies**—SAXS measurements were performed with a HECUS S3-Micro SAXS camera attached to a Xenocs microbeam delivery system (copper target, wavelength  $\lambda = 1.54$  Å) operating at a power of 50 watts. SAXS measurements of PrP samples with and without Cu<sup>2+</sup> (2 mg/ml in water (pH 7.4)) at 37 °C for 10,800 s were recorded with a Pilatus 100k pixel detector. The two-dimensional image was reduced to a one-dimensional scattering curve using the Fit2D software and processed using PRIMUS (37). The *R*<sub>g</sub> and *I*(0) values were obtained using the Guinier approximation (38). To obtain shape information, the scattering data were converted to *P*(*r*) function by GNOM software, and the *D*<sub>max</sub> was calculated (39). The *P*(*r*) function was taken to GASBOR, to generate *ab initio* models (40). This process was repeated 10 times and then averaged using DAMAVER (41). The high resolution NMR data of prion protein and the *ab initio* SAXS envelopes of PrP in the absence and presence of Cu<sup>2+</sup> obtained from GASBOR program were matched using SUPCOMB (42).

## RESULTS

**Reversible Aggregation of PrP(23–231) upon Cu<sup>2+</sup>-binding**—We measured aggregation of PrP upon Cu<sup>2+</sup>-binding by monitoring light scattering of the solution under physiological conditions (temperature 37 °C and pH 7.4). Six molar equivalents of Cu<sup>2+</sup> in the form of Cu(Gly)<sub>2</sub> (see under “Experimental Procedures”) were added to full-length PrP (Fig. 1A). No changes in the scattering at 37 °C were observed upon Cu<sup>2+</sup>-binding to PrP(23–231), indicating the absence of aggregation at this temperature (see Fig. 1A, before 200 s). We made a serendipitous observation that as the temperature was lowered to 15 °C, there was a sudden increase in the scattering, suggesting protein aggregation (200–400 s). When the temperature was raised back to 37 °C, the observed light scattering suddenly decreased (400–600 s), indicating reversible protein aggregation. The extent of reversibility was monitored by continuous heating and cooling of the sample for 14 times (supplemental Fig. S2A). The aggregation was reversible except for a minor decrease in the observed light scattering. Temperature dependence of this process (supplemental Figs. S1, A and B, and S2A) suggests that the aggregation occurs below 20 °C. However, at higher concentrations of PrP(23–231), the protein aggregates at higher temperatures (below 25 °C). We also observed that the extent of reversible aggregation increased with increasing concentration of PrP(23–231) (supplemental Fig. S1, C and D). Although this aggregation occurs at a nonphysiological temperature, a detailed understanding of this process is likely to provide insights into the molecular basis of Cu<sup>2+</sup>/PrP interac-

## Cu<sup>2+</sup>-PrP, Aggregation, and N- and C-terminal Interactions

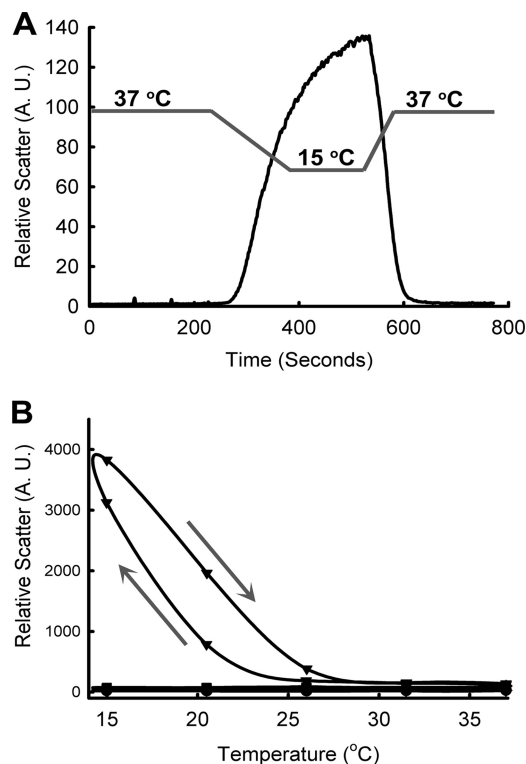


**FIGURE 1. Temperature-dependent reversible aggregation of Cu<sup>2+</sup>-bound PrP.** *A*, reversible aggregation of PrP(23–231) in the presence of Cu<sup>2+</sup>. Gray lines indicate temperature of the sample, and slopes of lines indicate decrease or increase in the temperature. *B*, reversible aggregation of similar concentrations of PrP(23–231) (circles), Cu<sup>2+</sup>-bound PrP(23–231) (triangles), PrP(90–231) (diamonds), and Cu<sup>2+</sup>-bound PrP(90–231) (squares). The circles, diamonds, and squares are overlapping. Arrows show the directions of experiments. Arrow pointing downward shows cooling, and arrow pointing upward shows heating of sample.

tion. We have therefore investigated the temperature-dependent, reversible aggregation of Cu<sup>2+</sup>-bound PrP.

To examine the role of electrostatic interactions in the Cu<sup>2+</sup>-bound PrP(23–231) aggregation, we monitored the protein aggregation at varying concentrations of salt (sodium chloride, NaCl) (supplemental Fig. S1, E and F). The extent of aggregation increased with an increase in salt concentration, suggesting the involvement of nonelectrostatic interactions such as hydrogen bonds (H-bonds) and hydrophobic interactions in the PrP(23–231) aggregation. PrP(23–231) binds Cu<sup>2+</sup> in the N-terminal region involving four octapeptide repeats (residues 60–91) and at the sites His-96 and His-111 (2–12). To probe the region(s) responsible for temperature-dependent aggregation of Cu<sup>2+</sup>-bound PrP(23–231), we have generated an N-terminal deletion mutant PrP(90–231), which lacks the four octapeptide repeats (region 23–89). Interestingly, Cu<sup>2+</sup>-bound PrP(90–231) (Fig. 1*B*, squares) did not show any aggregation, whereas the Cu<sup>2+</sup>-bound PrP(23–231) shows reversible aggregation as expected (Fig. 1*B*, triangles). This result shows that the region encompassing octapeptide repeats is responsible for the temperature-dependent reversible aggregation of Cu<sup>2+</sup>-bound PrP.

We used an amyloid-specific fluorescent probe thioflavin T (43) to further understand the nature of these aggregates (amyloid or amorphous). We did not observe any change in thioflavin T fluorescence with Cu<sup>2+</sup>-bound PrP(23–231) at various

temperatures (16, 20, 25, 30, and 37 °C), indicating that the aggregates formed are amorphous in nature (supplemental Fig. S2*B*). This result rules out any amyloidogenic conversion of PrP(23–231) upon Cu<sup>2+</sup>-binding in the given temperature range.

**Binding Affinity of Cu<sup>2+</sup> to PrP(23–231) at Various Temperatures**—It is possible that the observed temperature-dependent aggregation could be due to temperature-dependent changes in the affinity of Cu<sup>2+</sup> for PrP. We determined the affinity of Cu<sup>2+</sup> for PrP(23–231) at different temperatures using ITC. The apparent dissociation constants ( $K_{d(\text{app})}$ ) thus obtained from the curve fitting of base-line-corrected isotherms (see “Experimental Procedures”) did not show significant differences at various temperatures (statistical analysis shows *p* values in the range 0.11 to 0.23) (supplemental Fig. S2*C*). This result clearly suggests that the Cu<sup>2+</sup>-induced reversible aggregation of PrP(23–231) cannot be attributed to changes in the binding affinities.

The ITC data suggest that both  $\Delta H$  and  $\Delta S$  show linear changes with temperature (Fig. 2, A and B); although  $\Delta H$  decreased,  $\Delta S$  increased with temperature, indicating conformational changes associated with Cu<sup>2+</sup>-binding to PrP(23–231). Interestingly, we observed a linear correlation between  $\Delta H$  and  $\Delta S$  with a slope of 297.8 K (Fig. 2*C*). Such a linear and positive correlation between  $\Delta H$  and  $\Delta S$ , with a slope of  $\sim 300$  K, has been proposed to indicate enthalpy/entropy compensation for small solutes and proteins in water solutions (44, 45). Temperature-dependent compensation requires heat capacity to remain more or less constant throughout the temperature range used (46). In the present case, the calculated molar heat capacity indeed was found to be constant ( $\sim 517$  cal/mol/K, see Fig. 3*D*). This observation may be taken to suggest that at high temperatures the process is entropy-driven, whereas at lower temperatures it is driven by enthalpy.

**Novel Interactions between the N- and C-terminal Regions upon Cu<sup>2+</sup>-binding**—Isothermal titration calorimetry studies, *inter alia*, show positive and large heat capacity change upon Cu<sup>2+</sup>-binding to PrP(23–231) ( $\sim 517$  cal/mol/K, see Fig. 2*D*). Several studies associate positive and large heat capacity change with the breaking of H-bonds or long range electrostatic interactions or loss of polar residues on the surface- or temperature-dependent conformational changes (47). In our experiments, positive and large heat capacity change suggests that PrP(23–231) undergoes conformational changes upon binding to Cu<sup>2+</sup> at various temperatures. We have investigated the possible structural alteration using NMR and SAXS. Because PrP is a glycosylphosphatidylinositol-anchored protein, it has been suggested by Nishina *et al.* (48) that it is likely to exist in relatively nonpolar micro-environments with a dielectric constant similar to those of low ionic strength buffer solutions. We have therefore carried out these experiments under low ionic strength conditions (see “Experimental Procedures”). We have recorded a series of <sup>15</sup>N-<sup>1</sup>H HSQC spectra of PrP(23–231) (full length) at different temperatures in the presence and absence of Cu<sup>2+</sup> (Fig. 3; supplemental Fig. S3). We could monitor cross-peaks from the C-terminal region of PrP (residues 120–231). The cross-peaks from the N-terminal region (residues 23–120), which included Cu<sup>2+</sup>-binding sites such as the octapeptide

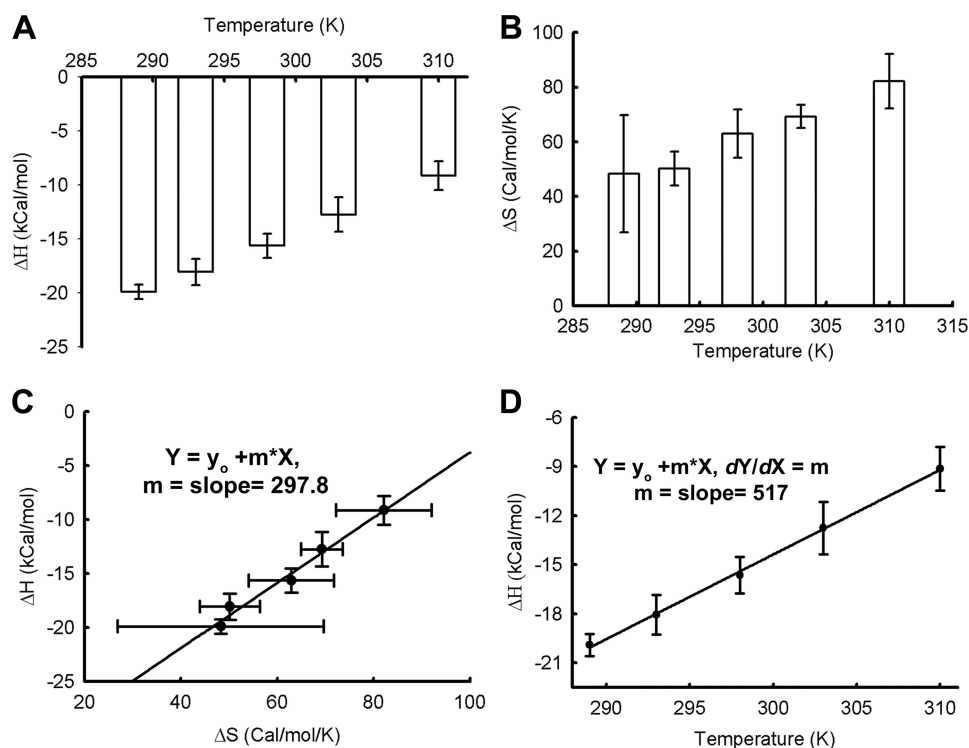


FIGURE 2. **Calorimetric studies on binding of  $\text{Cu}^{2+}$  to PrP.** A,  $\Delta H$ ; B,  $\Delta S$  of  $\text{Cu}^{2+}$ -binding to PrP at different temperatures. C, plot of  $\Delta H$  and  $\Delta S$ . Enthalpy/entropy compensation was observed in the case of  $\text{Cu}^{2+}$ -binding to PrP at various temperatures. Data were fitted with the linear equation ( $y = m \cdot x + C$ ), yielding a slope of 297.8 K. D, plot of  $\Delta H$  and  $T$ ; slope yields heat capacity change ( $\sim 517$  cal/mol/K). For all figures, S.E. was calculated using three sets of experiments.

repeats region (residues 60–91) and His-96/His-111, were not visible in the given spectra in the presence and absence of  $\text{Cu}^{2+}$  (see “Experimental Procedures”). This facilitated observation of specific conformational changes in the C-terminal region of PrP(23–231) induced by  $\text{Cu}^{2+}$ -binding to the N-terminal region. Being paramagnetic in nature,  $\text{Cu}^{2+}$  is known to increase transverse (spin-spin) relaxation rates, thereby broadening the NMR spectral lines (49). Upon  $\text{Cu}^{2+}$  addition, we observed the line broadening of only some but not all the peaks, indicating strong binding of  $\text{Cu}^{2+}$  to specific sites. Several of the original peaks in the HSQC spectrum of PrP(23–231) broadened, upon addition of  $\text{Cu}^{2+}$ , although others remained unaffected in their line widths. The intensities of these broadened peaks were below the NMR detection limit (Fig. 3). We further noted that the number of broadened cross-peaks increased with a decrease in temperature in the HSQC spectra of  $\text{Cu}^{2+}$ -bound PrP(23–231) (compare *blue cross-peaks* in Fig. 3A with those in B and those in [supplemental Fig. S3, A and F](#)). However, in the absence of  $\text{Cu}^{2+}$ , no such broadening of cross-peaks was noticed in the HSQC spectra of PrP(23–231) (compare *red* (without  $\text{Cu}^{2+}$ ) and *blue* (with  $\text{Cu}^{2+}$ ) *cross-peaks* in Fig. 3, A and B). At 37 °C, cross-peaks arising from Phe-141, Asn-143, and Asp-147 were found missing (Fig. 3A; Table 1; and Fig. 4, C, D, and F). As the temperature was lowered, peaks arising from Glu-146 and Ile-139 disappeared at 34 and 31 °C, respectively (Fig. 4, E and B; Table 1). Residues Ile-139 to Asn-143 correspond to the loop region preceding helix-1, whereas Glu-146 and Asp-147 are part of helix-1 (Fig. 4A). In addition to the above-mentioned residues, some of the peaks arising from the helix-2 region (residues 171–188) also showed line broadening

at temperatures below 37 °C (Table 1; Fig. 5, B–H). Asn-174 and Asp-178 were the first residues whose spectral signatures disappeared at 34 °C (Fig. 5, B and C). This was followed by the disappearance of peaks of Val-180 and Asn-181 at 31 °C (Fig. 5, E and F) and also Cys-179, Ile-182, and Lys-185 at 28 °C (Fig. 5, D, G, and H; Table 1).

Proximity of paramagnetic  $\text{Cu}^{2+}$  could lead to the line broadening (disappearance of peaks) in the HSQC spectra listed in Table 1. Formation of higher order assemblies, however, can also lead to line broadening. The results from the scattering experiments ([supplemental Fig. S1, A and B](#)) show that PrP(23–231) does not undergo aggregation in the presence of  $\text{Cu}^{2+}$  at these temperatures. We carried out dynamic light scattering measurements (under conditions identical to NMR experiments) and found no change in the hydrodynamic radius of PrP and  $\text{Cu}^{2+}$ -bound PrP ([supplemental Fig. S2D](#)). We also carried out sedimentation velocity measurements with PrP and  $\text{Cu}^{2+}$ -bound PrP at 37 °C. Fig. 6, A and B, shows the movement of sedimenting boundary, represented as fringe displacement with time, of the samples of PrP and  $\text{Cu}^{2+}$ -bound PrP, respectively. Fig. 6C shows the sedimentation coefficient profiles of PrP ( $s_{20,w}$ , 2.694) and  $\text{Cu}^{2+}$ -bound PrP ( $s_{20,w}$ , 2.862) derived from curve-fitting analyses of the sedimentation profiles. Sedimentation profiles indicate that  $\sim 98.5\%$  of the population in the samples containing PrP and  $\text{Cu}^{2+}$ -bound PrP are in monomeric form with a molecular mass of  $\sim 23.4$  kDa. The remaining negligible fraction ( $\sim 1.5\%$ ), which corresponds to higher oligomers (including dimers, trimers, or tetramers), is observed both in PrP and  $\text{Cu}^{2+}$ -bound PrP, clearly showing that addition of  $\text{Cu}^{2+}$  to PrP

## Cu<sup>2+</sup>-PrP, Aggregation, and N- and C-terminal Interactions

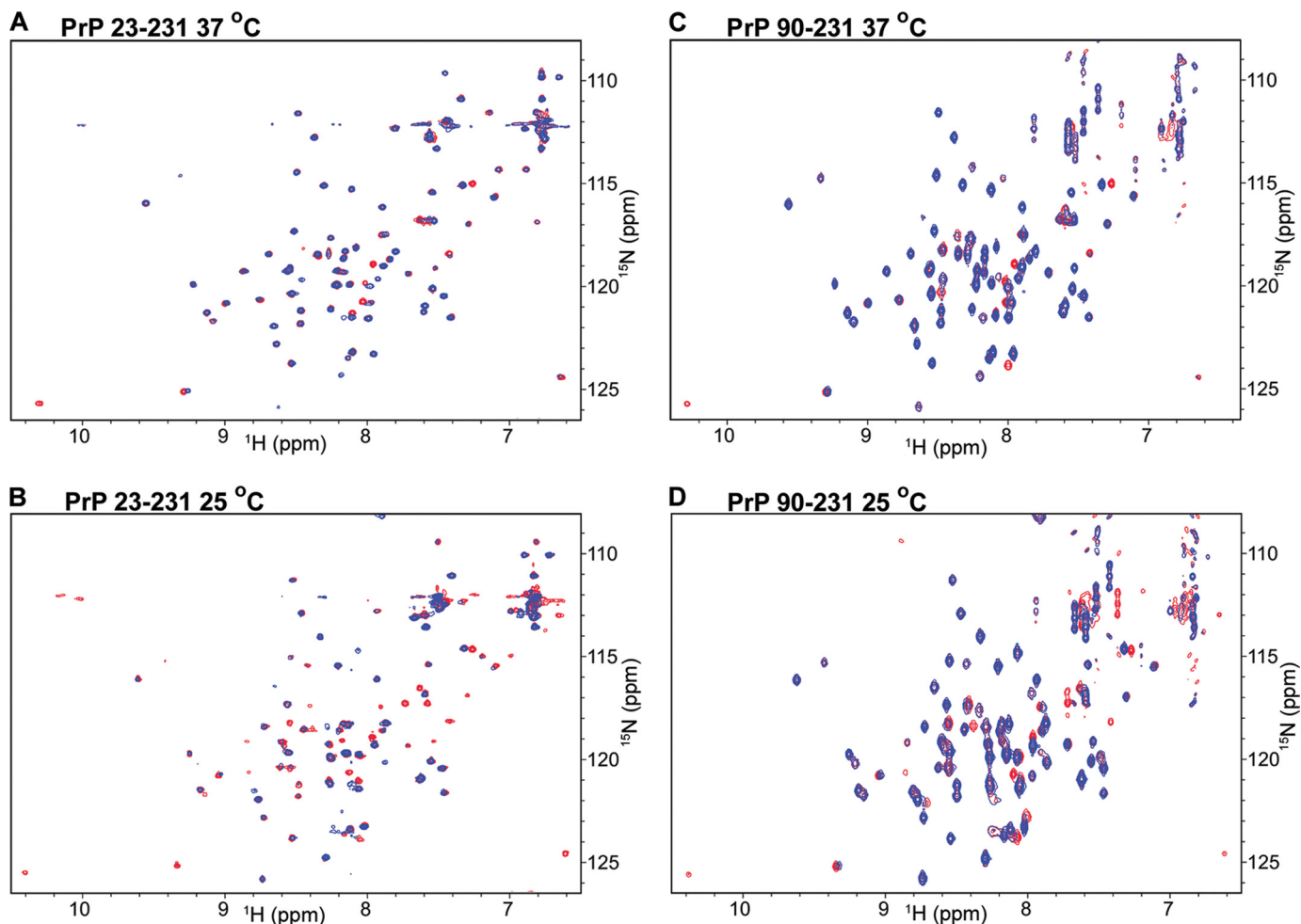


FIGURE 3. **Two-dimensional <sup>15</sup>N-<sup>1</sup>H HSQC spectra of PrP(23–231) and PrP(90–231).** A and B, two-dimensional <sup>15</sup>N-<sup>1</sup>H HSQC spectra of PrP(23–231) (red cross-peaks) were overlaid with those of Cu<sup>2+</sup>-bound PrP(23–231) (blue cross-peaks) at 37 °C (A) and 25 °C (B). C and D, two-dimensional <sup>15</sup>N-<sup>1</sup>H HSQC spectra of PrP(90–231) (red cross-peaks) and Cu<sup>2+</sup>-bound PrP(90–231) (blue cross-peaks) were at 37 °C (C) and 25 °C (D).

**TABLE 1**

**Lists of residues whose cross-peaks are missing upon addition of Cu<sup>2+</sup> at various temperatures**

In the two-dimensional <sup>15</sup>N-<sup>1</sup>H HSQC spectra of Cu<sup>2+</sup>-bound PrP(23–231), cross-peaks of these residues are broadened at a particular temperature compared with that of PrP(23–231). Cross-peaks of the residues (boldface) are also found to be missing in the HSQC spectra of Cu<sup>2+</sup>-bound PrP(90–231). In the case of Cu<sup>2+</sup>-bound PrP(90–231), cross-peak arising from Ile-139 disappeared at 25 °C in contrast to that of PrP(23–231), where it disappeared at 31 °C. Below 24 °C, cross-peaks are broadening due to the aggregation process, which is prevalent at or below 22 °C (shown in supplemental Table S1). Except Asp-178, residues in boldface belong to the helix-1 region and others correspond to the helix-2 region.

37 °C	34 °C	31 °C	28 °C
Ala-120 <sup>a</sup>	Ala-120	Ala-120	Ala-120
Phe-141	Phe-141	Phe-141	Phe-141
Asn-143	Asn-143	Asn-143	Asn-143
Asp-147	Asp-147	Asp-147	Asp-147
	Glu-146	Glu-146	Glu-146
	Asn-174	Asn-174	Asn-174
	Asp-178	Asp-178	Asp-178
	<b>Ile-139<sup>b</sup></b>	<b>Ile-139<sup>b</sup></b>	<b>Ile-139<sup>b</sup></b>
	Cys-180	Cys-180	Cys-180
	Asn-181	Asn-181	Asn-181
		Cys-170	Cys-170
		Ile-182	Ile-182
		Lys-185	Lys-185
		Arg-208 <sup>a</sup>	Arg-208 <sup>a</sup>

<sup>a</sup> Ala-120 is present in a flexible N-terminal region, and Arg-208 is present in helix-3.

<sup>b</sup> In the case of PrP(90–231), the cross-peak arising from Ile-139 was found to disappear at 25 °C.

samples at 37 °C does not lead to the formation of higher order assemblies. It is important to note that the sedimentation velocity and dynamic light scattering measurements were carried out under the same conditions of concentration of PrP, pH, and temperature as used in the NMR experiments. All these observations taken together clearly show that proximity of paramagnetic Cu<sup>2+</sup>, but not the formation of higher order assemblies, is responsible for the observed line broadening in HSQC spectra.

Interestingly, none of the residues in helix-1 and its nearby loop region (Ile-139–Asp-147) are implicated in Cu<sup>2+</sup>-binding to PrP. It is worth mentioning here that in the polypeptide stretch Ile-139 to Asp-147, His-140, not detected in the absence or presence of Cu<sup>2+</sup> in the given HSQC spectrum, is the lone residue that could bind Cu<sup>2+</sup>. However, studies by Van Doorslaer and co-workers (33) have clearly ruled out the possibility of Cu<sup>2+</sup>-binding at this residue. Therefore, we believe that the reason for the disappearance of peaks from these regions can only be explained if Cu<sup>2+</sup> bound at other sites such as the octapeptide repeats region and/or His-96/His-111 of the N-terminal region might become proximal to these residues and thus cause the paramagnetic line broadening leading to the disappearance of their spectral signatures.

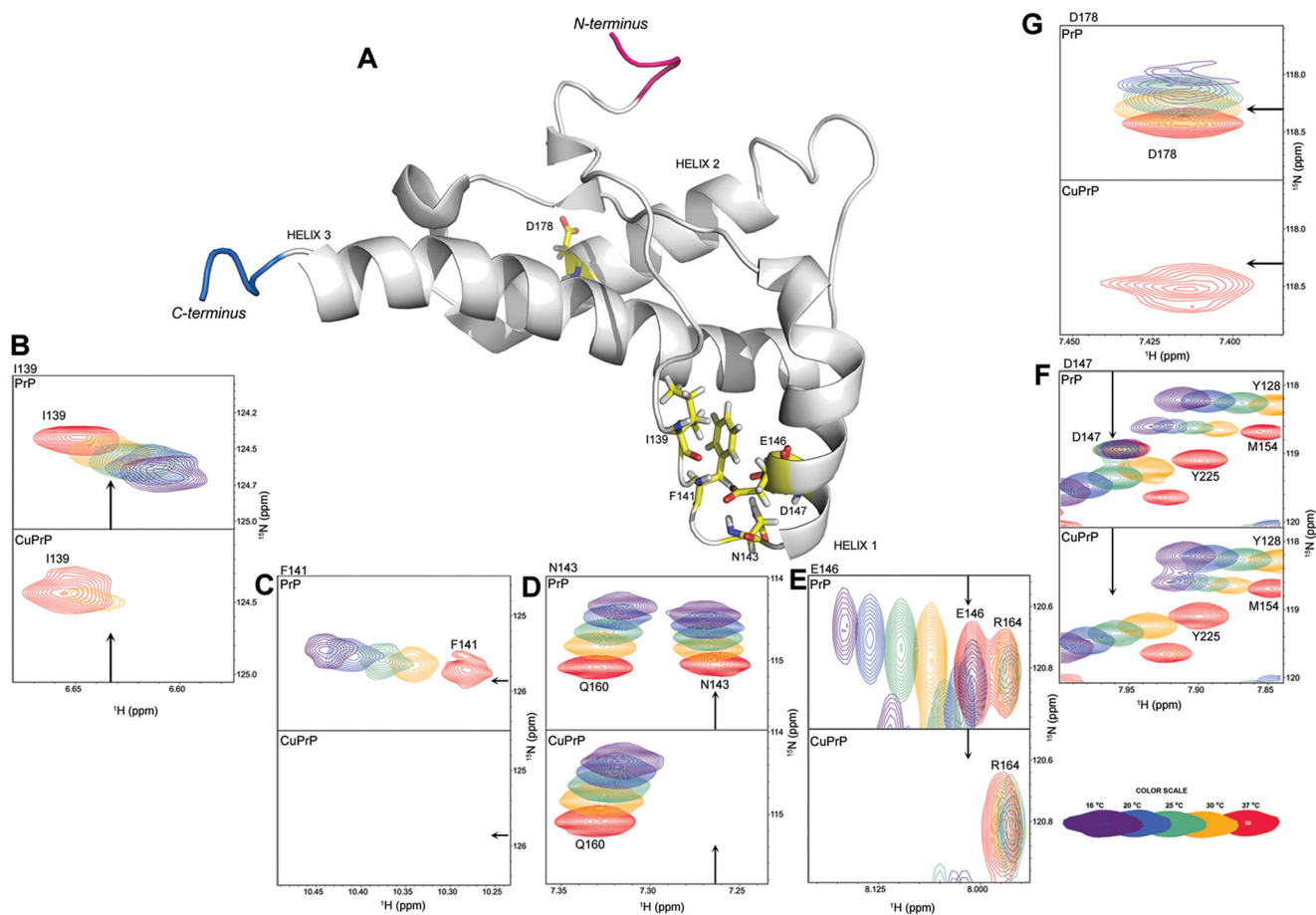


**FIGURE 4. Representation of the residues corresponding to missing cross-peaks in helix-1 of PrP(23–231) and PrP(90–231).** A, NMR structure of PrP(121–231) (BioMagResBank code 16071 and Protein Data Bank code 1XYX) displaying residues (in sticks with yellow backbone) from helix-1 and its nearby loop region, whose cross-peaks were found missing upon addition of  $\text{Cu}^{2+}$  to PrP(23–231) and PrP(90–231) in the temperature range of 37–24 °C. The cross-peaks of helix-1 residues Ile-139 (B), Phe-141 (C), Asn-143 (D), Glu-146 (E), Asp-147 (F), and helix-2 residue Asp-178 (G) in the absence of  $\text{Cu}^{2+}$  (upper panel) are compared with the cross-peaks obtained in the presence of  $\text{Cu}^{2+}$  (lower panel). Each panel has five different color cross-peaks that correspond to the same residues obtained at different temperatures from 16 °C (dark purple) to 37 °C (red) as shown in the color cross-peaks bar (bottom right corner). In each panel an arrow is used to indicate the approximate position of cross-peaks in the absence and presence of  $\text{Cu}^{2+}$ . Asp-178 is the only residue in helix-2 whose cross-peaks were found to be missing at and above 30 °C in the two-dimensional  $^{15}\text{N}$ - $^1\text{H}$  HSQC of  $\text{Cu}^{2+}$ -bound PrP(90–231). Residues are numbered according to the human PrP sequence. Val-121 and Ser-231 are the N-terminal (red) and C-terminal (blue) residues, respectively.

To probe residues from the N-terminal regions that might interact with helix-1 and helix-2 of the C-terminal region, we have recorded  $^{15}\text{N}$ - $^1\text{H}$  HSQC spectra of the N-terminal deletion mutant PrP(90–231), which lacks the four octapeptide repeats (region 23–89) leaving His-96/His-111, as the only  $\text{Cu}^{2+}$ -binding site. We noticed that the cross-peaks arising from Phe-141, Asn-143, Glu-146, Asp-147, and Asp-178 completely disappeared upon addition of  $\text{Cu}^{2+}$  at 37 °C (Figs. 3C and 4, C–G). Upon lowering the temperature to 25 °C, the cross-peak arising from Ile-139 also disappeared (Figs. 3D and 4B; supplemental Fig. S4B; in Table 1 see the **boldface** residues). Interestingly, the cross-peaks of PrP(90–231) from helix-1 and its nearby loop region (Ile-139–Asp-147), which broadened in the presence of  $\text{Cu}^{2+}$  at 37 °C, were similar to those of PrP(23–231), as mentioned above. PrP(90–231) did not show protein aggregation in the presence of  $\text{Cu}^{2+}$  at low temperatures (Fig. 1B). We therefore propose here that the C-terminal region (Ile-139 to Asp-147) of PrP is involved in a novel interaction with the  $\text{Cu}^{2+}$ -bound N-terminal region (residues 90–120 that contains the site His-96/His-111). The role of the octapeptide repeats in this interaction is less pronounced as  $\text{Cu}^{2+}$ -bound

PrP(90–231) does not have residues from 23 to 89 that harbor octapeptide repeats. Thus, on the basis of our observations in proteins PrP(90–231) and PrP(23–231), we suggest that the region 90–120 (which contains the site His-96/His-111) becomes proximal to the region Ile-139–Asp-147 for interaction, upon binding to  $\text{Cu}^{2+}$ .

PrP(23–231) also shows broadened cross-peaks from the helix-2 region, which is not observed in the case of PrP(90–231). A few reports suggest that  $\text{Cu}^{2+}$  binds to His-187 (9–12). However, we found that the cross-peak arising from His-187 broadened only below 22 °C in the HSQC spectra of  $\text{Cu}^{2+}$ -bound PrP(23–231) but not in that of  $\text{Cu}^{2+}$ -bound PrP(90–231) (Table S1). Because both the variants of PrP (PrP(23–231) and PrP(90–231)) have His-187, they should have shown a similar broadening phenomenon if  $\text{Cu}^{2+}$  binds to this site. Moreover, the broadened cross-peaks arising from the helix-2 region (residues 174–182 until 28 °C) are distal to His-187. Thus, the NMR data clearly shows that His-187 is not involved in  $\text{Cu}^{2+}$ -binding under the chosen experimental conditions. This observation indicates the presence of  $\text{Cu}^{2+}$  in close proximity of the helix-2 region, which might be responsible for the observed line

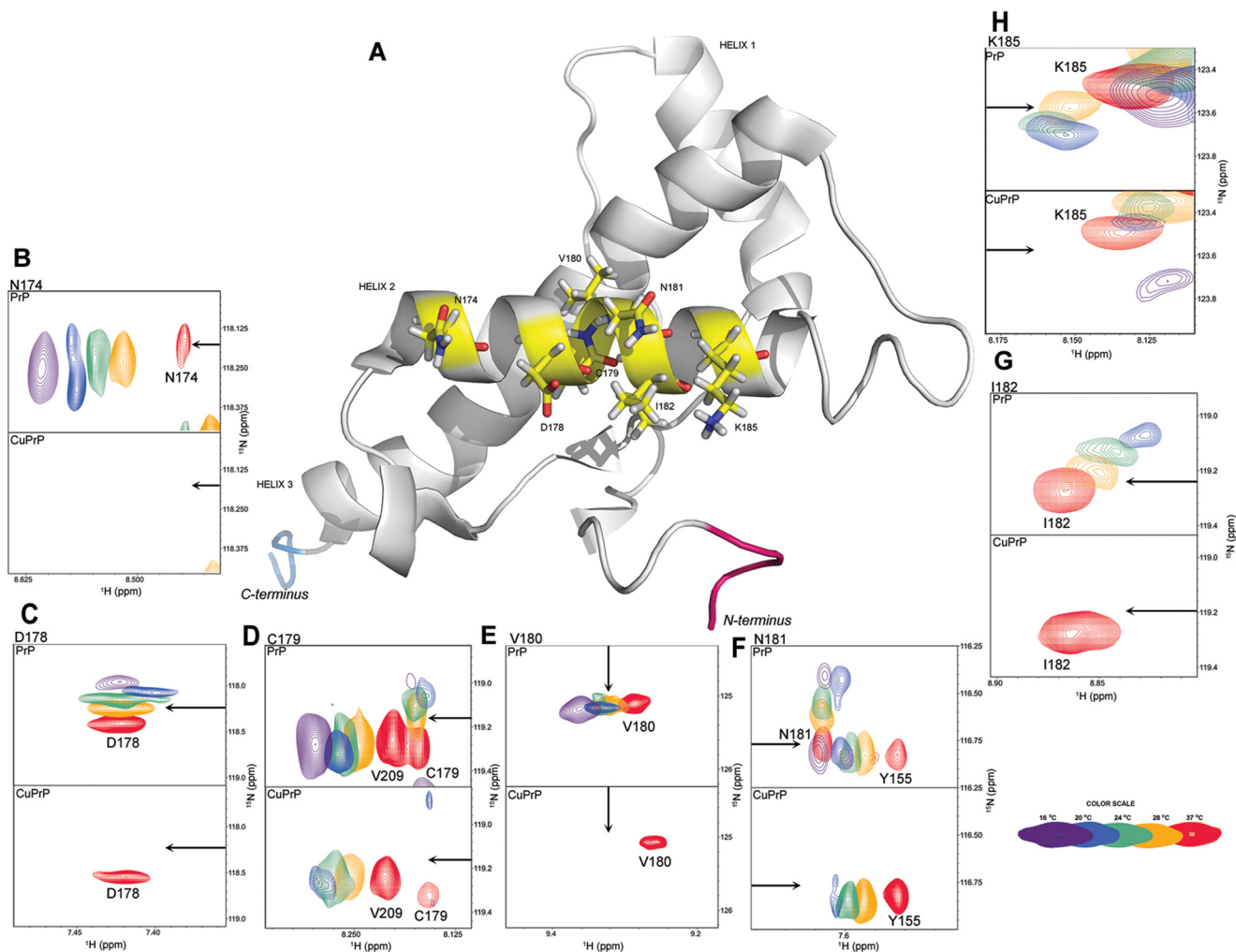


**FIGURE 5. Representation of the residues corresponding to missing cross-peaks in the helix-2 of PrP(23–231).** A, NMR structure of PrP(121–231) (BioMagResBank code 16071 and Protein Data Bank code 1XYX) displaying residues from helix-2 whose cross-peaks were found missing upon addition of  $\text{Cu}^{2+}$  to PrP(23–231) in the temperature range of 37–24 °C. The cross-peaks of these residues, Asn-174 (B), Asp-178 (C), Cys-179 (D), Val-180 (E), Asn-181 (F), Ile-182 (G), and Lys-185 (H), in the absence of  $\text{Cu}^{2+}$  (upper panel) are compared with those obtained in the presence of  $\text{Cu}^{2+}$  (lower panel). Each panel has five different color cross-peaks that correspond to the same residues obtained at different temperatures from 16 °C (dark purple) to 37 °C (red) as shown in the color cross-peaks bar (bottom right corner). In each panel an arrow is used to indicate approximate position of cross-peaks in the absence and presence of  $\text{Cu}^{2+}$ . Residues are numbered according to the human PrP sequence. Val-121 and Ser-231 are the N-terminal (red) and C-terminal (blue) residues, respectively.

broadening. We believe that the reason for the disappearance of peaks from this region can only be explained by a second novel interaction of the N-terminal domain with the helix-2 region. In the case of PrP(90–231) (which lacks octapeptide repeats), we did not observe broadening of peaks in the helix-2 region suggesting the role of  $\text{Cu}^{2+}$ -bound octapeptide repeats in the disappearance of cross-peaks from the helix-2 region. Therefore, we further propose that  $\text{Cu}^{2+}$ -bound octapeptide repeats region (residues 60–91) interacts with the helix-2 region (residues 174–185) and is responsible for the broadening of cross-peaks arising from this region. Viles *et al.* (28) investigated a small region of PrP covering 51–91 residues that harbor the  $\text{Cu}^{2+}$ -binding octapeptide repeats region and observed line broadening of some lines from this region. Because we have used full-length PrP(23–231), we were able to observe long range, intra-protein interactions upon  $\text{Cu}^{2+}$ -binding.

Our NMR results also show that residues present in hydrophobic core were less affected until 24 °C. Upon further lowering the temperature to 22 °C and below,  $\text{Cu}^{2+}$ -bound PrP(23–

231) exhibited protein aggregation. HSQC spectra recorded at these temperatures showed general broadening of cross-peaks originating from residues of helices 1 and 2 (supplemental Table S1) and a few of the residues belonging to helix-3, which are in contact with these helices. As described earlier, the octapeptide repeats are responsible for the temperature-dependent reversible aggregation of  $\text{Cu}^{2+}$ -bound PrP(23–231). On the basis of NMR results, we suggest the role of interaction of helix-2 and octapeptide repeats region in the temperature-dependent reversible aggregation of  $\text{Cu}^{2+}$ -bound PrP(23–231).

*Compaction of the Extended Conformation of PrP upon  $\text{Cu}^{2+}$ -binding*—Our results indicate that the line broadening of the peaks from helix-1 and helix-2 regions above 24 °C is not due to the formation of higher order assemblies but a result of the interaction of  $\text{Cu}^{2+}$ -bound N-terminal region with the C-terminal region of PrP(23–231).

To get an insight into these intra-molecular interactions of the N-terminal region with the C-terminal counterpart, we estimated  $R_g$  and  $D_{\text{max}}$  of PrP(23–231) and  $\text{Cu}^{2+}$ -bound



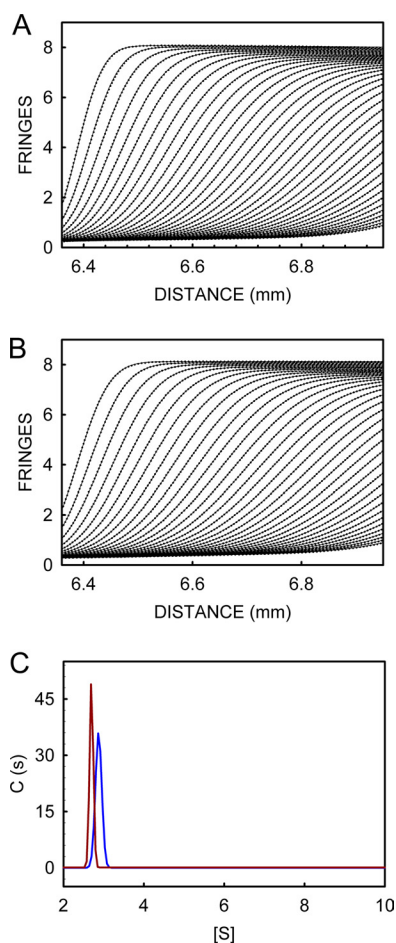


FIGURE 6. **Sedimentation velocity profiles of PrP and Cu<sup>2+</sup>-bound PrP.** Movement of sedimentary boundary as monitored using interference pattern of PrP (A) and Cu<sup>2+</sup>-bound PrP (B). C, sedimentation coefficient distribution of PrP (red) and Cu<sup>2+</sup>-bound PrP (blue).

PrP(23–231) using SAXS. The  $R_g$  of PrP(23–231) (2.55 nm) and Cu<sup>2+</sup>-bound PrP(23–231) (2.46 nm) determined by Guinier analysis show small differences (*left inset*, Fig. 7A). Distance distribution function,  $P(r)$  analysis, reveals reduction in the  $D_{\max}$  value from 10 nm for PrP(23–231) to 9 nm for Cu<sup>2+</sup>-bound PrP(23–231) (Fig. 7B), which suggests that Cu<sup>2+</sup>-bound PrP(23–231) might have become more compact compared with PrP. The N-terminal region of PrP is unstructured and flexible in nature. Hence, we analyzed the data using ensemble optimization method (EOM), which gives useful information such as  $R_g$  and  $D_{\max}$  distributions (50, 51) in the case of proteins with flexible domains. Fig. 7, C and D, compare the  $D_{\max}$  and  $R_g$  distributions, respectively, of the ensembles of the selected conformations with the  $D_{\max}$  and  $R_g$  distributions of the initial pool (randomly generated) of 10,000 structures. The  $D_{\max}$  and  $R_g$  distributions of PrP(23–231) and Cu<sup>2+</sup>-bound PrP(23–231) showed multimodal distributions. To discern these distribution curves, we have deconvoluted the  $D_{\max}$  and the  $R_g$  distribution plots (*supplemental Fig. S5, A–D*). In the  $D_{\max}$  distribution of PrP(23–231), the two conformer populations (mean around 7.31 and 9.52 nm with fractional contributions of 48.7 and 49.9%, respectively) (Fig. 7C, *red trace*; *supplemental Fig. S5B*) converged into a major population with  $D_{\max}$  8.39 nm (72.7%) upon Cu<sup>2+</sup>-binding (Fig. 7C, *blue trace*; *supplemental Fig.*

*S5D*). This suggests that a significant amount of compaction of the extended conformation of PrP(23–231) occurs upon Cu<sup>2+</sup>-binding. We also found similar features in the  $R_g$  distributions of PrP(23–231) and Cu<sup>2+</sup>-bound PrP(23–231).  $R_g$  distributions of PrP(23–231) corresponding to 2.25 nm (46.4%) and 3.05 nm (34.5%) (Fig. 7D, *red trace*; *supplemental Fig. S5A*) are changed to 2.24 nm (22.8%) and 2.65 nm (73.4%) (Fig. 7D, *blue trace*; *supplemental Fig. S5C*), respectively, upon Cu<sup>2+</sup>-binding, which supports the  $D_{\max}$  distribution data obtained above. The results from the EOM analysis of the size distribution are in agreement with the values obtained from  $P(r)$  distribution function, where reduction of 1 nm is seen for  $D_{\max}$  of Cu<sup>2+</sup>-bound PrP(23–231) compared with that of PrP(23–231). The reduction in the  $D_{\max}$  leading to the global compactness of Cu<sup>2+</sup>-bound PrP(23–231) might be the result of a decrease in the flexibility of the N-terminal region, which exhibits interaction with the C-terminal region of PrP(23–231) upon Cu<sup>2+</sup>-binding. Study from Viles *et al.* (28) suggests that upon Cu<sup>2+</sup>-binding the octapeptide repeats region achieves compact structure due to four coordinating histidine residues. Studies from Takeuchi *et al.* (52) have reported that Cu<sup>2+</sup> induces helix formation in the octapeptide repeat region (53). However, in both these studies short peptides comprising octapeptide or the repeat region (residues 51–91) have been used. We report here a global compaction of full-length PrP(23–231) due to inter-domain interactions upon Cu<sup>2+</sup>-binding. Thus, our SAXS results lend credence to the existence of long range interactions between the N- and C-terminal regions in the Cu<sup>2+</sup>-bound PrP(23–231). The observed marginal increase (Fig. 6C) in the sedimentation coefficient of Cu<sup>2+</sup>-bound PrP (2.86 from 2.69 for PrP) also indicates global compaction.

## DISCUSSION

We have observed temperature-dependent reversible aggregation of Cu<sup>2+</sup>-bound PrP(23–231); it aggregates at lower temperatures and resolubilizes at physiological temperature. We believe that a novel interaction between helix-2 and the octapeptide repeats region of PrP(23–231) is involved in this reversible aggregation. Our study further suggests that the aggregation might proceed through the formation of hydrogen bonds (H-bonds), which might dissociate rendering the PrP(23–231) soluble at physiological temperature. We have investigated the conformational consequences of Cu<sup>2+</sup>-binding to PrP(23–231) under physiological conditions. On the basis of our results, we propose novel interactions between the N- and C-terminal regions involving the flexible region and the helices-1 and -2.

*Aggregation of Cu<sup>2+</sup>-bound PrP—Cu<sup>2+</sup>* is known to play a role in prion diseases. It is shown to promote and prevent the process. We noticed that most of the Cu<sup>2+</sup>-binding experiments are either performed at nonphysiological temperatures (2, 10, 13–17) or at very high concentrations of Cu<sup>2+</sup> (54, 55). Under physiological conditions, we find that Cu<sup>2+</sup>-bound PrP(23–231) does not aggregate. Interestingly, it starts to aggregate when the temperature is lowered. Aggregation at lower temperature has been reported earlier (2, 10, 13–17). Our results suggest that Cu<sup>2+</sup> may not play a role in the aggregation of PrP at physiological temperature (37 °C). Our experiments with mutant protein (PrP(90–231)) show that the region

## Cu<sup>2+</sup>-PrP, Aggregation, and N- and C-terminal Interactions

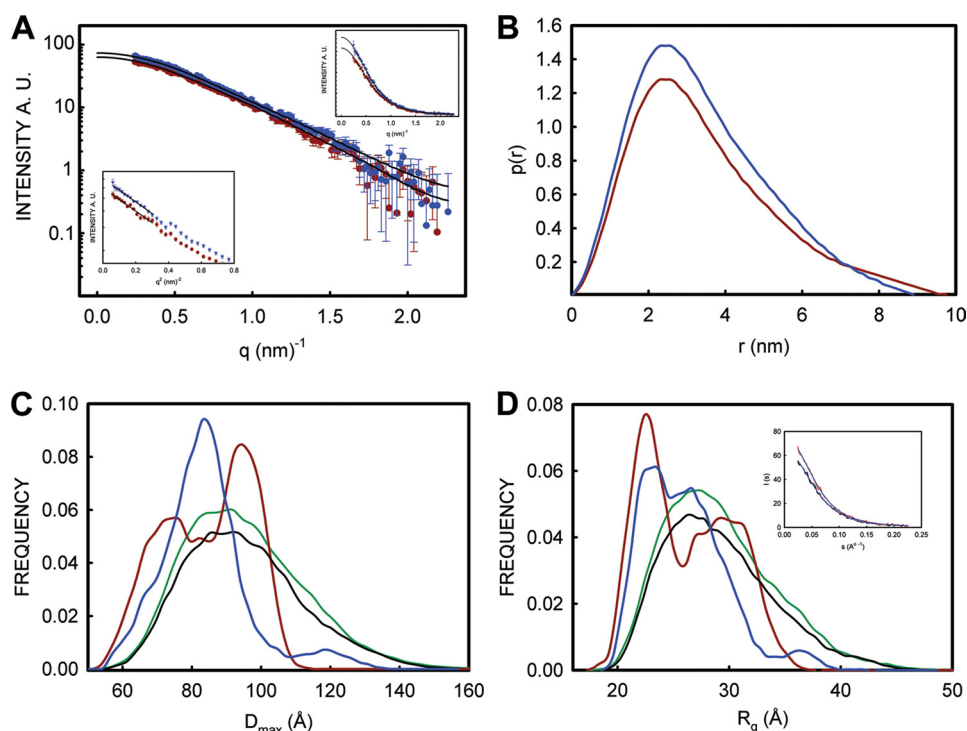


FIGURE 7. **SAXS measurements of PrP and Cu<sup>2+</sup>-bound PrP.** *A*, scattering profiles of PrP (red circles) and Cu<sup>2+</sup>-bound PrP (blue circles) plotted against  $q$  ( $q = 4\pi\sin\theta/\lambda$ ). Black traces are fitted lines obtained from  $P(r)$  distribution function. Differences in the scatter profiles of PrP and Cu<sup>2+</sup>-bound PrP are better seen in the linear plot (top right inset). Left bottom panel shows Guinier plots ( $\ln(I(q))$  versus  $q^2$ ) of PrP (red circle) and Cu<sup>2+</sup>-bound PrP (blue triangle). Straight lines show regions of the curve from where  $R_g$  values were calculated using Guinier plot. *B*, distance distribution function ( $P(r)$  function) of PrP (red trace) and Cu<sup>2+</sup>-bound PrP (blue trace). *C*,  $D_{\max}$ ; *D*,  $R_g$  distribution function calculated from the scattering profiles of PrP(23–231) (red trace in *A*) and Cu<sup>2+</sup>-bound PrP (blue trace in *A*) using the EOM method. In each (*C* and *D*), black traces show  $D_{\max}$  (*C*) and  $R_g$  (*D*) distributions calculated from the pool of 10,000 conformations from PrP scattering profiles and green traces are from those of Cu<sup>2+</sup>-bound profiles. Red trace in each panel shows distribution from the selected 20 structures from PrP scattering profiles, and blue trace shows that of Cu<sup>2+</sup>-bound PrP. *D*, inset, EOM fitting of the PrP (black over blue trace) and Cu<sup>2+</sup>-bound PrP (black over red trace) with  $\chi$  values of 0.778 and 0.775, respectively.

encompassing octapeptide repeats (residues 60–91) is responsible for the temperature-dependent reversible aggregation of Cu<sup>2+</sup>-bound PrP(23–231) (Fig. 1). Our ITC experiments show that the observed temperature-dependent aggregation might not be due to changes in the affinity of Cu<sup>2+</sup>-binding. Binding affinity remains invariant; however, enthalpy and entropy changes show linear and reciprocal relation indicating an enthalpy-entropy-compensation phenomenon (44, 45). The observed enthalpy/entropy compensation phenomenon might be useful in understanding the temperature-dependent aggregation; due to higher entropy at 37 °C, the Cu<sup>2+</sup>-binding sites will be flexible and solvated and might disrupt any cohesive inter-molecular interactions. This facilitates Cu<sup>2+</sup>-bound PrP(23–231) to remain in solution at 37 °C. However, at lower temperatures, these sites might come together initiating cohesive interactions via H-bonds or hydrophobic interactions. Hydrophobic interactions are known to increase in strength with increasing temperatures (56). As mentioned earlier, we observed that Cu<sup>2+</sup>-bound PrP(23–231) aggregates at low temperature, but not at higher temperature (supplemental Figs. S1, A and B, and S2A), indicating a rather lesser role for hydrophobic interactions in the process. Thus, we believe that H-bonds might play a prominent role in the temperature-dependent aggregation of Cu<sup>2+</sup>-bound PrP(23–231).

**Interaction between the N- and C-terminal Regions**—The possibility of interaction between the N- and C-terminal regions of PrP(23–231) has been indicated in earlier studies.

Binding of antibodies specific to the N- and C-terminal regions (57), high pressure (58), and NMR studies indicates the presence of a transient interaction of the C-terminal region of helix-2 (residues 187–193) and helix-3 (residues 217–226) with the unfolded N-terminal domain (34). Our Cu<sup>2+</sup>-binding studies using ITC revealed changes in enthalpy with temperatures that resulted in large positive heat capacity change. Large heat capacity change reflects structural rearrangements upon Cu<sup>2+</sup>-binding to PrP(23–231). Our NMR studies indicate previously unknown interactions of the N-terminal region with the C-terminal region in the Cu<sup>2+</sup>-bound PrP(23–231). The NMR of full-length PrP has been reported earlier; there are also reports of NMR studies on Cu<sup>2+</sup>-binding to fragments of PrP (28, 32, 59). To the best of our knowledge, this is the first investigation of NMR of Cu<sup>2+</sup>-bound full-length PrP, which shows novel long range inter-domain interactions.

Fig. 8 schematically describes temperature-dependent reversible aggregation and long range inter-domain interactions observed with Cu<sup>2+</sup>-bound PrP(23–231). PrP (Fig. 8, panel 1) shows interaction of the N-terminal region with the C-terminal region at helix-2 and -3 (residues 187–193 and 217–226, respectively) (green arrow) as reported earlier (55–57). At 37 °C, upon Cu<sup>2+</sup> addition, our studies suggest interaction of the N-terminal flexible domain with helix-1 and its nearby loop region (Fig. 8, panel 2, blue arrow). To the best of our knowledge, this is the first report of the interaction of helix-1 and its nearby region (residues 139–147) with the flexible N-terminal

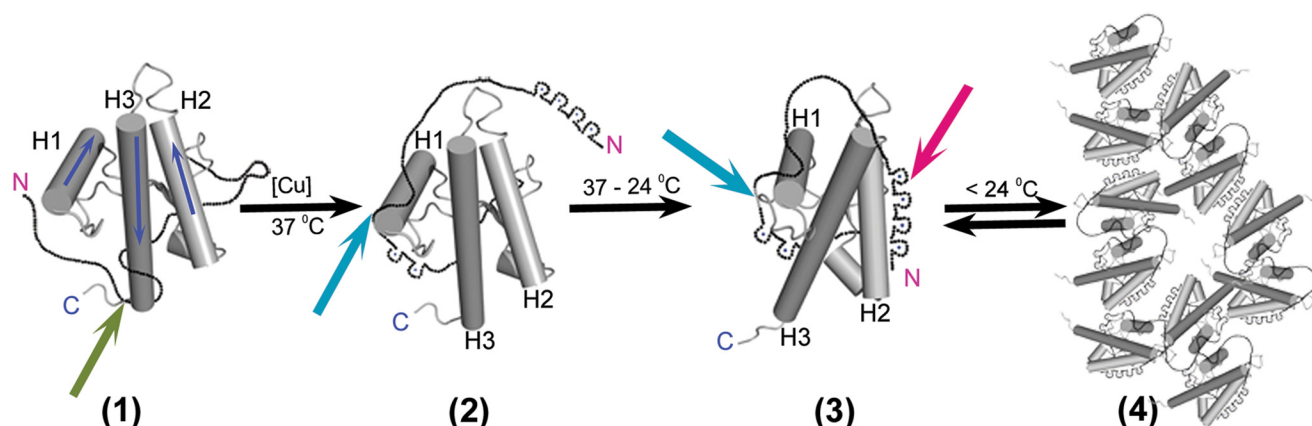


FIGURE 8. **Schematic model for novel interactions and  $\text{Cu}^{2+}$ -induced temperature-dependent aggregation of prion protein.** Panel 1, helices 1–3 are represented as H1, H2, and H3, respectively. Blue arrow in each helix shows the direction of helix. N (red) and C (blue) represents the N and C terminus of PrP. Green arrow in panel 1 describes transient interaction of the N with C terminus reported earlier in the absence of  $\text{Cu}^{2+}$  (see “Discussion” for details). Blue arrow in panels 2 and 3 shows interaction of the N-terminal region (90–120) with helix-1 and its nearby loop region (139–147) in the presence of  $\text{Cu}^{2+}$  obtained from our results. Red arrow in panel 3 shows interaction of octapeptide repeat region (60–91) with helix-2(174–185) upon  $\text{Cu}^{2+}$  addition. Below 24 °C,  $\text{Cu}^{2+}$ -bound PrP undergoes reversible aggregation (panel 4) via inter-molecular interaction initiated by interaction between octapeptide repeats region and helix-2. Structures are not to scale. Structural features are adopted from the NMR structure (Protein Data Bank code 1XYX) using PyMol software.

region (residues 90–120 that contains the site His-96/His-111).  $\text{Cu}^{2+}$ -bound PrP(23–231), in the temperature range 37–24 °C, exhibits another novel interaction between the N-terminal (residues 60–91) and the C-terminal (residues 174–185) regions in the presence of  $\text{Cu}^{2+}$  (Fig. 8, panel 3, red arrow). Aggregation at lower temperatures might be initiated via interaction of helix-2 and the  $\text{Cu}^{2+}$ -bound octapeptide repeats region. This interaction will further result in aggregation of  $\text{Cu}^{2+}$ -bound PrP (Fig. 8, panel 4).

Our SAXS results lend credence to the scheme described in Fig. 8. We have generated low resolution *ab initio* SAXS models for PrP(23–231) and  $\text{Cu}^{2+}$ -bound PrP(23–231) (supplemental Fig. S6).  $\text{Cu}^{2+}$ -bound PrP(23–231) (orange envelope) shows more curved and smaller envelope compared with that of PrP(23–231) (blue envelope) (supplemental Fig. S6, A and B). It is possible that the interaction of the flexible N-terminal region with the C-terminal region, upon  $\text{Cu}^{2+}$ -binding, leads to the observed changes in the shape of envelope of  $\text{Cu}^{2+}$ -bound PrP(23–231) compared with that of PrP(23–231).

**Functional Consequence of Interaction of Helix-1 and N-terminal Region (Residues 90–120)**—We believe that the interaction of the N-terminal region (residues 90–120 that contain the site His-96/His-111) with the C-terminal region (residues 139–147) is important because of the role played by helix-1 and its nearby loop in the conversion of PrP<sup>C</sup> to PrP<sup>SC</sup>. Involvement of helix-1 in the conversion of PrP<sup>C</sup> to PrP<sup>SC</sup> was first predicted by Morrissey and Shakhnovich(60) using CHARMM energy calculation. The  $\beta$ -nucleation model proposed by them states that PrP<sup>SC</sup> is an aggregate with a hydrophilic core, consisting of a  $\beta$ -sheet-like arrangement of constituent helix-1 components (60). Helix-1 has been shown to promote aggregation (61, 62). It was also found in the dimer interface of the crystal structure of human PrP (63). Site 139–141 has been shown to be the most pressure-sensitive region (58) and found to have a much higher aggregation tendency compared with helix-1 (64). The helix-1 region Asn-143–Glu-146 also plays a prominent role in the prion conversion *in vivo* (65). Thus, it is evident that helix-1 and the nearby loop region play a major role in the aggregation and

conversion of PrP to PrP<sup>SC</sup>. Our study shows that helix-1 and the nearby loop region interact with the N-terminal region (residues 90–120 that contain the site His-96/His-111) upon  $\text{Cu}^{2+}$ -binding. As mentioned earlier,  $\text{Cu}^{2+}$  inhibits amyloid formation of PrP *in vitro* (22). Baskakov and co-workers (22) attributed this inhibition to binding of  $\text{Cu}^{2+}$  in the C-terminal region of PrP. However, even in the absence of the C-terminal region, PrP(82–146), in the presence of  $\text{Cu}^{2+}$ , did not show amyloid fibril formation (23). It is possible that the interaction of the N-terminal region (residues 90–120) with the loop (Ile-139–Phe-141) and helix-1 (Asn-143–Arg-148) region of PrP(23–231) upon  $\text{Cu}^{2+}$ -binding is responsible for the observed inhibition of the amyloid fibril formation in all the three cases, namely PrP(82–146) (23), PrP(89–231) (22), and PrP(23–231) (22). This interaction is not present in PrP(23–231) in the absence of  $\text{Cu}^{2+}$ . We therefore propose an inhibitory role of  $\text{Cu}^{2+}$  on the conversion of PrP<sup>C</sup> to PrP<sup>SC</sup> *in vitro* and *in vivo* via the interaction between the N-terminal region and helix-1 and its nearby loop region.

**Functional Consequence of Interaction of Helix-2 and Octapeptide Repeats**—PrP(23–231), in contrast to PrP(90–231), undergoes temperature-dependent reversible aggregation upon  $\text{Cu}^{2+}$ -binding possibly because of the interaction between the octapeptide repeats region (residues 60–91) and helix-2. Reversible aggregation of  $\text{Cu}^{2+}$ -bound PrP(23–231) is only observed at lower temperature but not at 37 °C. Therefore, we believe that interaction between the octapeptide repeats region and the helix-2 region primes  $\text{Cu}^{2+}$ -bound PrP(23–231) for inter-protein interactions at 37 °C. Such interactions might have physiological significance.

The globular C-terminal domain of PrP includes two subdomains, H1-B1 and B2-H2-H3. NMR relaxation dynamics show that H1-B1 and the connecting loop are more flexible compared with the B2-H2-H3 subdomain (66). Rare, large scale motions of the subdomains have been proposed to initiate prion protein aggregation (67). Recent studies have shown that separation of these subdomains and formation of domain-swapped dimers are a prerequisite for the aggregation of prion

## Cu<sup>2+</sup>-PrP, Aggregation, and N- and C-terminal Interactions

protein (68, 69). This implies that increased proximity between these subdomains might have an opposite effect and might delay or completely abrogate the aggregation process. In this study, we show that N-terminal region wraps around C-terminal region by interacting with helix-1 and helix-2 upon copper binding. This might lead to increased proximity of the subdomains, thus inhibiting the aggregation process. It appears that copper inhibits amyloid formation either by interfering with the region comprising H1 and the nearby loop (see above) or by decreasing separation between the two subdomains of the C-terminal region. These implications are important in the context of amyloid formation and role of copper in prion disease.

Harris and Pauly (70) proposed that conformational changes in PrP<sup>C</sup> upon Cu<sup>2+</sup>-binding might increase the affinity of the protein for a putative endocytic receptor that localizes PrP<sup>C</sup> in clathrin-coated pits. Based on our observations, we propose that the interaction between the octapeptide repeats region and the helix-2 region might be responsible for the conformational changes required for increased endocytosis.

The role of Cu<sup>2+</sup> as an attenuator or facilitator in prion diseases is highly controversial. Our observation that PrP(23–231) in the presence of Cu<sup>2+</sup> does not aggregate at 37 °C supports the suggestion that Cu<sup>2+</sup> attenuates prion disease. However, we have also observed an unusual temperature-dependent aggregation of Cu<sup>2+</sup>-bound PrP(23–231). It aggregated at lower temperature and resolubilized at physiological temperature. We have investigated this phenomenon using various biophysical techniques such as ITC, NMR, and SAXS thus providing detailed thermodynamic and conformational aspects of Cu<sup>2+</sup>-binding to PrP(23–231). We observed two novel long range inter-domain interactions between the N- and C-terminal regions. Our study shows that Cu<sup>2+</sup>-bound His-96/His-111 becomes proximal to helix-1 and its nearby loop region (residues 139–147). This region is shown to have a prominent role in amyloidogenesis *in vitro* (22) and prion conversion *in vivo* (23). Our observation suggests that upon Cu<sup>2+</sup>-binding, the proximity of His-96/His-111 to Ile-139–Asp-147 and proximity between the two subdomains of the C-terminal region are involved in the inhibition of amyloid formation. In addition, we also observed interaction of the octapeptide repeats region (residues 60–91) with helix-2 (residues 174–185) upon Cu<sup>2+</sup>-binding. We speculate the involvement of this interaction in the aggregation process at lower temperatures. We believe that these interactions should prove useful in understanding the biological functions of prion protein upon Cu<sup>2+</sup>-binding *in vivo* such as conformational changes (71), endocytosis (70), lipid rafts localization, and Cu<sup>2+</sup>-induced signal transduction (72, 73) and in developing therapeutic strategies against prion diseases.

*Acknowledgments*—We thank T. Ramakrishna, T. K. Chowdary, Z. Kamal, and B. Raman for insightful discussion and critical reading of the manuscript. A. K. S. and K. V. R. C. acknowledge the facilities provided by the National Facility for High Field NMR, supported by Department of Science and Technology, Department of Biotechnology, Council of Scientific and Industrial Research, New Delhi, India, and Tata Institute of Fundamental Research, Mumbai, India.

## REFERENCES

1. Baldwin, M. A., Pan, K. M., Nguyen, J., Huang, Z., Groth, D., Serban, A., Gasset, M., Mehlhorn, I., Fletterick, R. J., and Cohen, F. E. (1994) *Philos. Trans. R. Soc. Lond. B Biol. Sci.* **343**, 435–441
2. Quaglio, E., Chiesa, R., and Harris, D. A. (2001) *J. Biol. Chem.* **276**, 11432–11438
3. Thompsett, A. R., Abdelraheim, S. R., Daniels, M., and Brown, D. R. (2005) *J. Biol. Chem.* **280**, 42750–42758
4. Badrick, A. C., and Jones, C. E. (2009) *J. Inorg. Biochem.* **103**, 1169–1175
5. Nadal, R. C., Davies, P., Brown, D. R., and Viles, J. H. (2009) *Biochemistry* **48**, 8929–8931
6. Brown, D. R., Qin, K., Herms, J. W., Madlung, A., Manson, J., Strome, R., Fraser, P. E., Kruck, T., von Bohlen, A., Schulz-Schaeffer, W., Giese, A., Westaway, D., and Kretzschmar, H. (1997) *Nature* **390**, 684–687
7. Jackson, G. S., Murray, I., Hosszu, L. L., Gibbs, N., Waltho, J. P., Clarke, A. R., and Collinge, J. (2001) *Proc. Natl. Acad. Sci. U.S.A.* **98**, 8531–8535
8. Hasnain, S. S., Murphy, L. M., Strange, R. W., Grossmann, J. G., Clarke, A. R., Jackson, G. S., and Collinge, J. (2001) *J. Mol. Biol.* **311**, 467–473
9. Cereghetti, G. M., Schweiger, A., Glockshuber, R., and Van Doorslaer, S. (2001) *Biophys. J.* **81**, 516–525
10. Brown, D. R., Guantieri, V., Grasso, G., Impellizzeri, G., Pappalardo, G., and Rizzarelli, E. (2004) *J. Inorg. Biochem.* **98**, 133–143
11. Colombo, M. C., Vandevondele, J., Van Doorslaer, S., Laio, A., Guidoni, L., and Rothlisberger, U. (2008) *Proteins* **70**, 1084–1098
12. Watanabe, Y., Hiraoka, W., Igarashi, M., Ito, K., Shimoyama, Y., Horiuchi, M., Yamamori, T., Yasui, H., Kuwabara, M., Inagaki, F., and Inanami, O. (2010) *Biochem. Biophys. Res. Commun.* **394**, 522–528
13. Jones, C. E., Abdelraheim, S. R., Brown, D. R., and Viles, J. H. (2004) *J. Biol. Chem.* **279**, 32018–32027
14. Tagliavini, F., Prelli, F., Verga, L., Giaccone, G., Sarma, R., Gorevic, P., Ghetti, B., Passerini, F., Ghibaudi, E., Forloni, G., et al. (1993) *Proc. Natl. Acad. Sci. U.S.A.* **90**, 9678–9682
15. Zahn, R. (2003) *J. Mol. Biol.* **334**, 477–488
16. Hodak, M., Chisnell, R., Lu, W., and Bernholc, J. (2009) *Proc. Natl. Acad. Sci. U.S.A.* **106**, 11576–11581
17. Qin, K., Yang, D. S., Yang, Y., Chishti, M. A., Meng, L. J., Kretzschmar, H. A., Yip, C. M., Fraser, P. E., and Westaway, D. (2000) *J. Biol. Chem.* **275**, 19121–19131
18. Stevens, D. J., Walter, E. D., Rodriguez, A., Draper, D., Davies, P., Brown, D. R., and Millhauser, G. L. (2009) *PLoS Pathog.* **5**, e1000390
19. Yu, S., Yin, S., Pham, N., Wong, P., Kang, S. C., Petersen, R. B., Li, C., and Sy, M. S. (2008) *FEBS J.* **275**, 5564–5575
20. Giese, A., Levin, J., Bertsch, U., and Kretzschmar, H. (2004) *Biochem. Biophys. Res. Commun.* **320**, 1240–1246
21. Orem, N. R., Geoghegan, J. C., Deleault, N. R., Kacsak, R., and Supattapone, S. (2006) *J. Neurochem.* **96**, 1409–1415
22. Bocharova, O. V., Breydo, L., Salnikov, V. V., and Baskakov, I. V. (2005) *Biochemistry* **44**, 6776–6787
23. Ricchelli, F., Buggio, R., Drago, D., Salmona, M., Forloni, G., Negro, A., Tognon, G., and Zatta, P. (2006) *Biochemistry* **45**, 6724–6732
24. Sigurdsson, E. M., Brown, D. R., Alim, M. A., Scholtzova, H., Carp, R., Meeker, H. C., Prelli, F., Frangione, B., and Wisniewski, T. (2003) *J. Biol. Chem.* **278**, 46199–46202
25. Hortells, P., Monleón, E., Acín, C., Vargas, A., Vasseur, V., Salomon, A., Ryyfel, B., Cesbron, J. Y., Badiola, J. J., and Monzón, M. (2010) *Zoonoses. Public Health* **57**, 358–366
26. Chattopadhyay, M., Walter, E. D., Newell, D. J., Jackson, P. J., Aronoff-Spencer, E., Peisach, J., Gerfen, G. J., Bennett, B., Antholine, W. E., and Millhauser, G. L. (2005) *J. Am. Chem. Soc.* **127**, 12647–12656
27. Aronoff-Spencer, E., Burns, C. S., Avdievich, N. I., Gerfen, G. J., Peisach, J., Antholine, W. E., Ball, H. L., Cohen, F. E., Prusiner, S. B., and Millhauser, G. L. (2000) *Biochemistry* **39**, 13760–13771
28. Viles, J. H., Cohen, F. E., Prusiner, S. B., Goodin, D. B., Wright, P. E., and Dyson, H. J. (1999) *Proc. Natl. Acad. Sci. U.S.A.* **96**, 2042–2047
29. Di Natale, G., Osz, K., Nagy, Z., Sanna, D., Micera, G., Pappalardo, G., Sívágó, I., and Rizzarelli, E. (2009) *Inorg. Chem.* **48**, 4239–4250
30. Osz, K., Nagy, Z., Pappalardo, G., Di Natale, G., Sanna, D., Micera, G.,

- Rizzarelli, E., and S3v3g3, I. (2007) *Chemistry* **13**, 7129–7143
31. Di Natale, G., Grasso, G., Impellizzeri, G., La Mendola, D., Micera, G., Mihala, N., Nagy, Z., Osz, K., Pappalardo, G., Rig3, V., Rizzarelli, E., Sanna, D., and S3v3g3, I. (2005) *Inorg. Chem.* **44**, 7214–7225
  32. Hornemann, S., von Schroetter, C., Damberger, F. F., and W3thrich, K. (2009) *J. Biol. Chem.* **284**, 22713–22721
  33. Cereghetti, G. M., Schweiger, A., Glockshuber, R., and Van Doorslaer, S. (2003) *Biophys. J.* **84**, 1985–1997
  34. Zahn, R., Liu, A., L3hrs, T., Riek, R., von Schroetter, C., L3pez Garc3a, F., Billeter, M., Calzolari, L., Wider, G., and W3thrich, K. (2000) *Proc. Natl. Acad. Sci. U.S.A.* **97**, 145–150
  35. Thakur, A. K., and Rao, ChM. (2008) *PLoS One* **3**, e2688
  36. Schuck, P. (2000) *Biophys. J.* **78**, 1606–1619
  37. Konarev, P. V., Volkov, V. V., Sokolova, A. V., Koch, M. H., and Svergun, D. I. (2003) *J. Appl. Crystallogr.* **36**, 1277–1282
  38. Guinier, A., and Fournet, G. (1955) *Small Angle Scattering of X-rays*, pp. 5–82, John Wiley & Sons, Inc., New York
  39. Svergun, D. I. (1992) *J. Appl. Crystallogr.* **25**, 495–503
  40. Svergun, D. I., Petoukhov, M. V., and Koch, M. H. (2001) *Biophys. J.* **80**, 2946–2953
  41. Volkov, V. V., and Svergun, D. I. (2001) *J. Appl. Crystallogr.* **36**, 860–864
  42. Kozin, M., and Svergun, D. I. (2000) *J. Appl. Crystallogr.* **34**, 33–41
  43. LeVine, H., 3rd (1999) *Methods Enzymol.* **309**, 274–284
  44. Lumry, R., and Rajender, S. (1970) *Biopolymers* **9**, 1125–1227
  45. Dunitz, J. D. (1995) *Chem. Biol.* **2**, 709–712
  46. Cooper, A., Johnson, C. M., Lakey, J. H., and N3llmann, M. (2001) *Biophys. Chem.* **93**, 215–230
  47. Sturtevant, J. M. (1977) *Proc. Natl. Acad. Sci. U.S.A.* **74**, 2236–2240
  48. Nishina, K., Jenks, S., and Supattapone, S. (2004) *J. Biol. Chem.* **279**, 40788–40794
  49. Banci, L., Pierattelli, R., and Vila, A. J. (2002) *Adv. Protein Chem.* **60**, 397–449
  50. Bernad3, P. (2010) *Eur. Biophys. J.* **39**, 769–780
  51. Bernad3, P., Mylonas, E., Petoukhov, M. V., Blackledge, M., and Svergun, D. I. (2007) *J. Am. Chem. Soc.* **129**, 5656–5664
  52. Miura, T., Hori-i, A., and Takeuchi, H. (1996) *FEBS Lett.* **396**, 248–252
  53. Brown, D. R., and Sassoon, J. (2002) *Mol. Biotechnol.* **22**, 165–178
  54. Tsirolnikov, K., Rezaei, H., Dalgalarondo, M., Chobert, J. M., Grosclaude, J., and Haertl3, T. (2006) *Biochim. Biophys. Acta* **1764**, 1218–1226
  55. Redecke, L., von Bergen, M., Clos, J., Konarev, P. V., Svergun, D. I., Fittschen, U. E., Broekaert, J. A., Bruns, O., Georgieva, D., Mandelkow, E., Genov, N., and Betzel, C. (2007) *J. Struct. Biol.* **157**, 308–320
  56. Chandler, D. (2005) *Nature* **437**, 640–647
  57. Li, R., Liu, T., Wong, B. S., Pan, T., Morillas, M., Swietnicki, W., O'Rourke, K., Gambetti, P., Surewicz, W. K., and Sy, M. S. (2000) *J. Mol. Biol.* **301**, 567–573
  58. Kachel, N., Kremer, W., Zahn, R., and Kalbitzer, H. R. (2006) *BMC Struct. Biol.* **6**, 16
  59. P3rez, D. R., Damberger, F. F., and W3thrich, K. (2010) *J. Mol. Biol.* **400**, 121–128
  60. Morrissey, M. P., and Shakhnovich, E. I. (1999) *Proc. Natl. Acad. Sci. U.S.A.* **96**, 11293–11298
  61. Watzlawik, J., Skora, L., Frense, D., Griesinger, C., Zweckstetter, M., Schulz-Schaeffer, W. J., and Kramer, M. L. (2006) *J. Biol. Chem.* **281**, 30242–30250
  62. Solfrosi, L., Bellon, A., Schaller, M., Cruite, J. T., Abalos, G. C., and Williamson, R. A. (2007) *J. Biol. Chem.* **282**, 7465–7471
  63. Knaus, K. J., Morillas, M., Swietnicki, W., Malone, M., Surewicz, W. K., and Yee, V. C. (2001) *Nat. Struct. Biol.* **8**, 770–774
  64. Ziegler, J., Viehrig, C., Geimer, S., R3sch, P., and Schwarzwinger, S. (2006) *FEBS Lett.* **580**, 2033–2040
  65. Norstrom, E. M., and Matrianni, J. A. (2006) *J. Virol.* **80**, 8521–8529
  66. Viles, J. H., Donne, D., Kroon, G., Prusiner, S. B., Cohen, F. E., Dyson, H. J., and Wright, P. E. (2001) *Biochemistry* **40**, 2743–2753
  67. Schwarzwinger, S., Horn, A. H., Ziegler, J., and Sticht, H. (2006) *J. Biomol. Struct. Dyn.* **23**, 581–590
  68. Eghiaian, F., Daubenfeld, T., Quenet, Y., van Audenhaege, M., Bouin, A. P., van der Rest, G., Grosclaude, J., and Rezaei, H. (2007) *Proc. Natl. Acad. Sci. U.S.A.* **104**, 7414–7419
  69. Hafner-Bratkovic, I., Bester, R., Pristovsek, P., Gaedtke, L., Veranic, P., Gaspersic, J., Mancek-Keber, M., Avbelj, M., Polymenidou, M., Julius, C., Aguzzi, A., Vorberg, I., and Jerala, R. (2011) *J. Biol. Chem.* **286**, 12149–12156
  70. Pauly, P. C., and Harris, D. A. (1998) *J. Biol. Chem.* **273**, 33107–33110
  71. Leclerc, E., Serban, H., Prusiner, S. B., Burton, D. R., and Williamson, R. A. (2006) *Arch. Virol.* **151**, 2103–2109
  72. Stuermer, C. A., Langhorst, M. F., Wiechers, M. F., Legler, D. F., Von Hanwehr, S. H., Guse, A. H., and Plattner, H. (2004) *FASEB J.* **18**, 1731–1733
  73. Monnet, C., Gavard, J., M3ge, R. M., and Sobel, A. (2004) *FEBS Lett.* **576**, 114–118